

# Atomic Alignment Effects for the Formation of Excimers RgX\* (B, C) in the Reaction of Oriented Rg ( $^3P_2$ , $M_J = 2$ ) (Rg = Xe, Kr, Ar) + Halogen(X)-Containing Molecules

H. Ohoyama,\* K. Yasuda, and T. Kasai

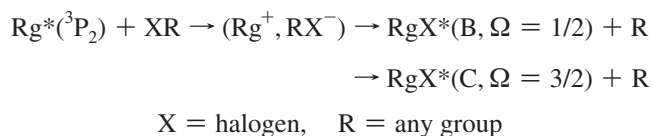
Department of Chemistry, Graduate School of Science, Osaka University Toyonaka, Osaka 560-0043, Japan

Received: May 27, 2009; Revised Manuscript Received: June 17, 2009

Atomic alignment effects for the formation of excimers, RgX\* (B,  $\Omega = 1/2$ ) and RgX\* (C,  $\Omega = 3/2$ ), in the reaction of Rg ( $^3P_2$ ) (Rg = Xe, Kr, Ar) with halogen (X)-containing molecules (RX) (CH<sub>3</sub>I, CF<sub>3</sub>I, CF<sub>3</sub>Br, NF<sub>3</sub>, CHBr<sub>3</sub>, CHCl<sub>3</sub>, CCl<sub>3</sub>F, and CCl<sub>4</sub>) have been measured by using an oriented Rg ( $^3P_2$ ,  $M_J = 2$ ) atomic beam at a collision energy of  $\sim 0.07$  eV. The emission intensities for RgX\* (B, C) have been measured as a function of the magnetic orientation field direction in the collision frame. The reactant (RX) dependence of the atomic alignment effect is extremely different between the RgX\* (B) and the RgX\* (C) channels. For RgX\* (C), an analogous atomic alignment effect is commonly observed despite the difference of RX and Rg. In contrast, for RgX\* (B), the atomic alignment effect shows a diverse dependence on RX and Rg.

## 1. Introduction

The reactions of Rg\* ( $^3P$ ) with polyatomic halogen-containing molecules RX are known to be similar to the reactions of alkali metal atoms, M. This similarity is due to the analogous outer valence electron configuration between Rg\* ( $(n-1)p^5ns^1$ ) and M ( $(n-1)p^6ns^1$ ).<sup>1</sup> The reaction of Rg\* generating electronically excited rare-gas halides RgX\* is known to proceed via the harpooning mechanism such as the formation of metal halide MX for the alkali metal atoms.<sup>2</sup> The formation of excimer RgX\* has been widely studied as a benchmark system for the harpooning mechanism.<sup>2–8</sup> Because the excited ion-pair potential  $V(\text{Rg}^+, \text{RX}^-)$  differs from that of the alkali metal atom case in terms of the effects related to the nonclosed shell nature of the positive ion-core Rg<sup>+</sup>, these ion cores should affect the exit channel potential and play an important role in controlling the branching to each reaction channel. The nonclosed shell of Rg<sup>+</sup> gives rise to two different excited rare gas halide product states, RgX\* (B) and RgX\* (C) that correlate with Rg<sup>+</sup> ( $^3P_{3/2}$ ) and X<sup>-</sup> ( $^1S_0$ ).



It is well known that the reactions of excited alkaline earth metal atoms M\* ( $(n-1)p^6ns^1np^1$ ) with polyatomic halogen-containing molecules also produce the electronically excited metal halide MX\* via the harpooning mechanism. The steric effects due to the nonclosed outer  $np$  shell in M\* have been studied. Rettner and Zare first studied the effect of atomic reagent approach geometry on reactivity with polarized laser for the reaction of Ca ( $^1P_1$ ) with HCl, Cl<sub>2</sub>, and CCl<sub>4</sub>.<sup>9</sup> Young et al. studied the orbital alignment effect for the reaction of Ca ( $^1P_1$ ) with CH<sub>4–n</sub>Cl<sub>n</sub> ( $n = 1$  to 4) reactions.<sup>10</sup> It was reported that the reaction of the Ca ( $^1P_1$ ) atom having a naked

outer atomic  $p$  orbital with CCl<sub>4</sub> displays no significant dependence on approach geometry. Lee et al. studied the orbital alignment dependence in collision of Ba( $^1P$ ) with NO<sub>2</sub> and O<sub>3</sub>.<sup>11</sup> The difference in the orbital configuration between Rg\* ( $(n-1)p^5ns^1$ ) and excited alkaline earth metal atoms M\* ( $(n-1)p^6ns^1np^1$ ) provides interesting contrast on the stereoselectivity. Despite the numerous studies on the RgX\* formation, the steric effect due to the nonclosed shell nature of the positive ion-core Rg<sup>+</sup> is still an unresolved problem.<sup>12</sup>

In the present study, we measured the atomic alignment effects for the formation of RgX\* (B) and RgX\* (C) in the reaction of oriented Rg ( $^3P_2$ ,  $M_J = 2$ ) (Rg = Xe, Kr, Ar) with halogen (X)-containing molecules (RX: CH<sub>3</sub>I, CF<sub>3</sub>I, CF<sub>3</sub>Br, NF<sub>3</sub>, CHBr<sub>3</sub>, CHCl<sub>3</sub>, CCl<sub>3</sub>F, and CCl<sub>4</sub>). A significant atomic alignment effect was observed for the RgX\* (B, C) formation. It was found that the reactant (RX) dependence of the atomic alignment effect is extremely different between the RgX\* (B) and RgX\* (C) channels. For RgX\* (C), an analogous atomic alignment effect is commonly observed despite the difference between RX and Rg. In contrast, for RgX\* (B), the atomic alignment effect shows a diverse dependence on RX and Rg. These atomic alignment effects are discussed by the  $\Omega_1$  conservation model which is based on the conservation of the  $\Omega'$  component in the course of ion-pair (Rg<sup>+</sup>–RX<sup>-</sup>) formation.

## 2. Experiment

The experimental apparatus and procedure were almost same as the previous one.<sup>13,14</sup> In brief, the metastable Rg ( $^3P_{0,2}$ ) (Rg = Xe, Kr, Ar) atomic beam was generated by a pulsed glow discharge with a pulse width of 100  $\mu\text{s}$ , and then the Rg ( $^3P_2$ ,  $M_J = 2$ ) state was selected by a magnetic hexapole. An almost pure Rg ( $^3P_2$ ,  $M_J = 2$ ) atomic beam with a velocity of 395  $\text{ms}^{-1}$  for Xe (490  $\text{ms}^{-1}$  for Kr, 700  $\text{ms}^{-1}$  for Ar) collides with the RX (CH<sub>3</sub>I, CF<sub>3</sub>I, CF<sub>3</sub>Br, NF<sub>3</sub>, CHBr<sub>3</sub>, CHCl<sub>3</sub>, CCl<sub>3</sub>F, and CCl<sub>4</sub>) molecular beam in a homogeneous magnetic orientation field, **B**. The RX molecular beam was injected with a stagnation pressure of 10 Torr from a pulsed valve that was placed at a distance of 8 cm from the beam crossing point. The chemilu-

\* Part of the “Vincenzo Aquilanti Festschrift”.

\* Corresponding author. E-mail: ohoyama@chem.sci.osaka-u.ac.jp.

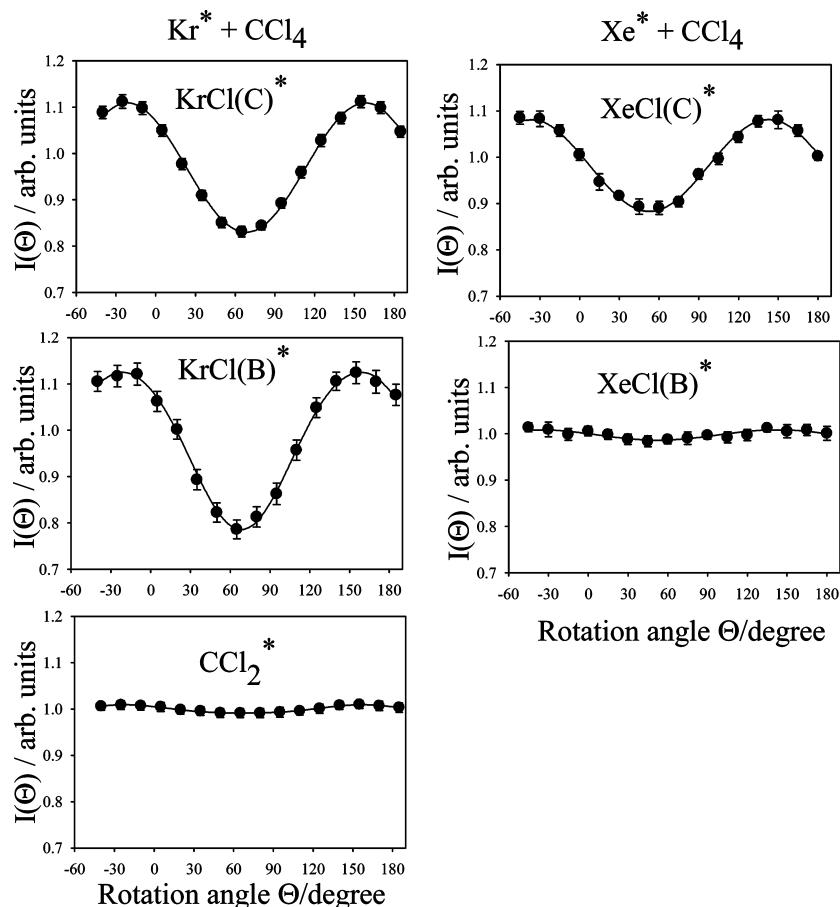


**Figure 1.** Chemiluminescence intensity as a function of the rotation angle,  $\Theta$ , of the magnetic orientation field direction for  $\text{RgCl}^*(\text{C})$ ,  $\text{RgCl}^*(\text{B})$ , and  $\text{CCl}_2^*(\text{A})$  in the reaction  $\text{Rg}({}^3\text{P}_2) + \text{CCl}_4$  ( $\text{Rg} = \text{Kr}, \text{Xe}$ ). Experimental ( $\bullet$ )  $\Theta$  dependence represented by the fittings using eq 4 (—). The origin of the rotational angle,  $\Theta$ , is the direction of the  $\text{Rg}({}^3\text{P}_2)$  atomic beam axis.

minescence from the each product,  $\text{RgX}^*(\text{B})$  and  $\text{RgX}^*(\text{C})$ , was selectively collected and detected by a photomultiplier through a suitable band-pass filter. Unfortunately, the  $\text{KrX}^*(\text{B})$  spectra are overlapped with the tail of  $\text{KrX}^*(\text{C})$  spectra for the reaction of  $\text{Kr}({}^3\text{P}_2) + \text{RX}$ . In such a case, the  $\text{KrX}^*(\text{B})$  signal was obtained as the difference signal between the whole excimer signal ( $\text{KrX}^*(\text{B}) + \text{KrX}^*(\text{C})$ ) and the  $\text{KrX}^*(\text{C})$  signal weighted by the branching ratio between the  $\text{KrX}^*(\text{B})$  and  $\text{KrX}^*(\text{C})$  channels.

The signal from a photomultiplier was counted by a multi-channel scaler (Stanford SR430). The  $\text{RgX}^*(\text{B}, \text{C})$  chemiluminescence intensity,  $I(\Theta)$ , was measured as a function of the magnetic orientation field direction in the laboratory frame (rotation angle  $\Theta$ ). The origin of  $\Theta$  is the direction of the  $\text{Rg}({}^3\text{P}_2)$  beam axis. The homogeneous magnetic orientation field was generated by the four pieces of ferrite magnets mounted on a motor-driven rotatable stage, and its direction  $\mathbf{B}$  was rotated around the beam crossing point over the angular range  $-45 \leq \Theta \leq 180^\circ$  by an interval of  $15^\circ$ .

### 3. Results and Discussion

**3.1. Atomic Alignment Effect.** In the present study, the  $\text{Rg}({}^3\text{P}_2, M_J = 2)$  atomic beam is oriented in a homogeneous magnetic orientation field,  $\mathbf{B}$ . For the collision processes, however, the relative velocity vector serves as the other relevant quantization axis. The cross section is then a function of the angle between those two quantization axes. In the following discussion, we use the notation of  $M_J$  for projec-

tions in the laboratory frame (the quantization axis is the magnetic orientation field,  $\mathbf{B}$ ). Primed symbols such as  $M_J'$  and  $\Omega'$  are used for projections in the collision frame. (The quantization axis is the relative velocity vector.)

As an example, the  $\Theta$  dependences of the chemiluminescence intensities of  $\text{RgCl}^*(\text{B}, \text{C})$  and  $\text{CCl}_2^*$  from the reaction of  $\text{Rg}({}^3\text{P}_2) + \text{CCl}_4$  ( $\text{Rg} = \text{Kr}, \text{Xe}$ ) are shown in Figure 1. A significant difference is observed between two excimer channels  $\text{RgCl}^*(\text{B}, \text{C})$  for  $\text{Kr}({}^3\text{P}_2)$  and  $\text{Xe}({}^3\text{P}_2)$ . These  $\Theta$ -dependences can be analyzed using an evolution procedure based on an irreducible representation of the density matrix.<sup>13</sup> In general, the  $\Theta$ -dependence of the emission intensity  $I(\Theta)$  can be expressed by

$$I(\Theta) = \frac{D\bar{I}}{(2J+1)} \sum_{kq} g_k(J) S_{kq}(B, J) T_{kq}(B, J) \quad (1)$$

where  $S_{kq}(B, J)$  and  $T_{kq}(B, J)$  are the real multipole moments of the density matrix of the prepared oriented  $\text{Rg}({}^3\text{P}_2, M_J = 2)$  atom and of the collision density matrix, respectively,  $D$  is an experimental detection efficiency,  $\bar{I}$  is the polarization averaged cross section, and  $g_k(J)$  are numerical factors.

In the present study, the general eq 1 can be simplified as the following equation by using the relative cross section of each magnetic substate,  $M_J'$ , in the collision frame,  $\sigma^{M_J'}$

$$I(\Theta) = \frac{1}{280}(39\sigma^{M_j=0} + 88\sigma^{M_j=1} + 153\sigma^{M_j=2}) + \frac{1}{16}(-3\sigma^{M_j=0} - 4\sigma^{M_j=1} + 7\sigma^{M_j=2}) \cos 2\theta \quad (2) + \frac{1}{64}(3\sigma^{M_j=0} - 4\sigma^{M_j=1} + \sigma^{M_j=2}) \cos 4\theta$$

This equation is equivalent to the general multipole moments form.

$$I(\Theta) = a_0 + a_2 \cos 2\theta + a_4 \cos 4\theta \quad (3)$$

where  $\theta$  is the angle between the relative velocity,  $v_R$ , and the direction of the orientation magnetic field,  $\mathbf{B}$ . It is defined as  $\theta \equiv \Theta_{v_R} - \Theta$  using the direction of the relative velocity  $v_R$  in the laboratory frame  $\Theta_{v_R}$ . Because  $\Theta_{v_R}$  has a distribution by the misalignment caused by the velocity distribution of the RX beam, we must use the  $\cos 2n\theta$  factors averaged over the Maxwell–Boltzmann velocity distribution of the RX beam at room temperature,  $\langle \cos(2n(\Theta_{v_R} - \Theta)) \rangle$ . We finally use the following equation for the evaluation of the experimental results

$$I_{\text{obsd}}(\Theta) = a_0 + a_2 \langle \cos(2(\Theta_{v_R} - \Theta)) \rangle + a_4 \langle \cos(4(\Theta_{v_R} - \Theta)) \rangle \quad (4)$$

The experimental measurements were fitted by a least-squares analysis with this equation to determine the  $a_n$  coefficients. These coefficients were used to derive the relative cross sections for each  $M_j$  state,  $\sigma^{M_j=0}$ ,  $\sigma^{M_j=1}$ , and  $\sigma^{M_j=2}$ . As a whole, it is found that the excimer formation is dominantly controlled by the alignment of the inner 5p electron of Xe ( $^3P_2$ ,  $M_j = 2$ ) (4p for Kr and 3p for Ar) in the collision frame because no notable  $a_4$  term is recognized for all reaction systems. In addition, the atomic alignment effect for the dissociative energy transfer process is observed to be negligible for all observable reaction systems. (See Figure 1.) This result indicates that both the electron transfer process for the formation of ion pair ( $\text{Rg}^+ - \text{RX}^-$ ) and the back electron transfer from the ion pair to the excited state have little atomic alignment effect.

The experimental atomic alignment effect (coefficient ratios,  $a_2/a_0$ ) for two excimer channels  $\text{RgX}^*$  (B, C) is reported in Figure 2. They are qualitatively summarized as follows.

**RgX\* (C) Channel.** (1) All reaction systems show a positive atomic alignment effect (positive  $a_2/a_0$  term). (2) A similar atomic alignment effect (constant  $a_2/a_0$  term) is observed for all reactants (RX) despite the large difference in the total quenching cross section and in the branching fraction. (3) The  $a_2/a_0$  term depends on Rg. The  $a_2/a_0$  term for the Kr ( $^3P_2$ ,  $M_j = 2$ ) system is larger than that for the Xe ( $^3P_2$ ,  $M_j = 2$ ) system.

**RgX\* (B) Channel.** (4) Atomic alignment effects show a variety of dependence on RX and Rg (positive and negative  $a_2/a_0$  term).

**Dissociative Energy Transfer.** No notable  $a_2/a_0$  term is recognized.

**3.2.  $\Omega'$ -Conservation in the Ion-Pair ( $\text{Rg}^+ - \text{RX}^-$ ) Formation.** Because the spin–spin coupling between the ion core of  $\text{Rg}^+ (^2P_{3/2})$  and the  $ns$  electron is weak as compared with the spin–orbit coupling in  $\text{Rg}^+ (^2P_{3/2})$ ,  $\text{Rg} (^3P_2)$  can be expressed as  $ns[3/2]_2^0$  by  $j-1$  coupling.<sup>5,6</sup> In this case, it is likely that the spin–orbit state of  $\text{Rg}^+ (^2P_j)$  after the electron jump of the  $ns$  electron becomes  $\text{Rg}^+ (^2P_{3/2})$  state. That is, the conservation of the ion core is expected after the electron jump of the  $ns$  electron. Indeed, no formation of  $\text{KrX}^*$  (C,  $\Omega = 3/2$ ) in the Kr ( $^3P_0$ ) +

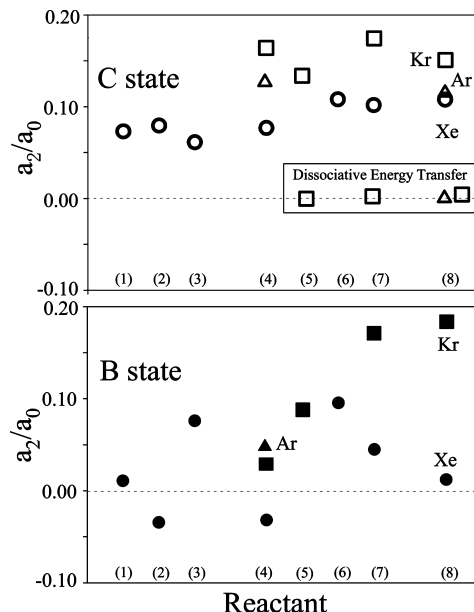
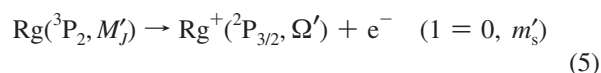


**Figure 2.** The  $a_2/a_0$  term (atomic alignment effect) for the formation of  $\text{RgX}^*$  (B) and  $\text{RgX}^*$  (C) in the reaction of oriented Rg ( $^3P_2$ ,  $M_j = 2$ ) (Rg = Xe (circle), Kr (square), and Ar (triangle)) with the halogen (X)-containing molecules RX ( $\text{CH}_3\text{I}$  (1),  $\text{CF}_3\text{I}$  (2),  $\text{CF}_3\text{Br}$  (3),  $\text{NF}_3$  (4),  $\text{CHBr}_3$  (5),  $\text{CHCl}_3$  (6),  $\text{CCl}_3\text{F}$  (7), and  $\text{CCl}_4$  (8)). The symbols in the inner box show the  $a_2/a_0$  term for the formation of excited products ( $\text{CCl}_2^*$  for  $\text{CCl}_3\text{F}$  (7) and  $\text{CCl}_4$  (8) and  $\text{CH}^*$  for  $\text{CHBr}_3$  (5)) from the dissociative energy transfer reaction of Kr ( $^3P_2$ ) and Ar ( $^3P_2$ ). The  $a_2/a_0$  terms were determined as the fitting parameters of the atomic alignment effect by the use of eq 2 through a  $\chi^2$  analysis. No notable  $a_4$  term is recognized in all reaction systems.

RX reaction due to the restriction from the conservation of spin–orbit state in the ion core ( $\text{Kr}^+ (^2P_{1/2})$ ) has been reported.<sup>2</sup> If the ion-core  $\text{Rg}^+ (^2P_{3/2})$  in the Rg ( $^3P_2$ ,  $M_j$ ) reactant is conserved after the electron jump of the  $ns$  electron, the configuration of angular momentum of  $\text{Rg}^+ (^2P_{3/2})$  provides two spin–orbit states,  $\Omega' = 3/2$  and  $1/2$ , in the collision frame



where  $m'_s$  is the magnetic spin quantum state of  $ns$  electron in the Rg ( $^3P_2$ ,  $M_j$ ).

A clear  $M_j$  effect observed in the  $\text{RgX}^*$  formation indicates that the formation of two spin–orbit states of  $\text{RgX}^*$  should be controlled by the configuration of the hole in the  $(n-1)p$  shell in the  $\text{Rg}^+ (^2P_{3/2})$  ion core of Rg ( $^3P_2$ ,  $M_j$ ) in the collision frame. In other words, the  $\Omega'$  component in the  $\text{Rg}^+ (^2P_{3/2})$  ion core of each Rg ( $^3P_2$ ,  $M_j$ ) state must be preserved into the configuration of the hole in the  $(n-1)p$  shell of  $\text{Rg}^+ (^2P_{3/2})$  in the ion pair ( $\text{Rg}^+ - \text{RX}^-$ ). Therefore, we can assume the conservation of  $\Omega'$  component in the course of ion-pair ( $\text{Rg}^+ - \text{RX}^-$ ) formation.

According to the  $\Omega'$  conservation in the course of ion-pair formation, the fraction of  $\Omega'$  component in each Rg ( $^3P_2$ ,  $M_j$ ) state,  $W_{\Omega'}(M_j)$ , can be calculated by using a standard recoupling procedure of angular momentum in terms of the Clebsch–Gordan coefficients for the case of  $J = 2$ ,  $j = 3/2$  (for the ion core), and  $s = 1/2$  (for the  $ns$  electron) as follows<sup>15</sup>

$$W_{\Omega'}(M_j) = |\langle 2, M_j | 3/2, \Omega' = (M_j - m'_s), 1/2, m'_s \rangle|^2 \quad (6)$$

They are shown in Figure 3. Because the  $\text{Rg}^+ (^2\text{P}_{3/2}, \Omega')$  core has two spin-orbit states,  $\Omega' = 3/2$  and  $1/2$ , in the collision frame, the  $M'_j$ -dependent cross section for the  $\text{RgX}^* (\Omega)$  formation generally can be expressed by

$$\sigma^\Omega(M'_j) = \sigma_{\Omega'=\Omega}^\Omega \times W_{\Omega'=\Omega}(M'_j) + \sigma_{\Omega' \neq \Omega}^\Omega \times W_{\Omega' \neq \Omega}(M'_j) \quad (7)$$

where  $\sigma_{\Omega'=\Omega}^\Omega$  is the cross section for the  $\Omega' = \Omega$  case ( $\text{RgX}^* (\Omega)$  formation from the configuration of  $\text{Rg}^+ (^2\text{P}_{3/2}, \Omega' = \Omega)$  in the collision frame), and  $\sigma_{\Omega' \neq \Omega}^\Omega$  is the cross section for the  $\Omega' \neq \Omega$  case ( $\text{RgX}^* (\Omega)$  formation from the configuration of  $\text{RgX}^+ (^2\text{P}_{3/2}, \Omega' \neq \Omega)$  in the collision frame). Indeed, the experimental  $M'_j$ -dependent cross sections can be well represented in this form. That is, we can express  $\sigma_{\Omega'=\Omega}^\Omega$  and  $\sigma_{\Omega' \neq \Omega}^\Omega$  by the following relationship

$$\sigma^{M'_j=2}(\Omega) = \sigma_{\Omega'=3/2}^\Omega, \quad \sigma^{M'_j=1}(\Omega) = 0.25 \times \sigma_{\Omega'=3/2}^\Omega + 0.75 \times \sigma_{\Omega'=1/2}^\Omega, \quad \sigma^{M'_j=0}(\Omega) = \sigma_{\Omega'=1/2}^\Omega \quad (8)$$

Therefore, from eq 2, we can determine

$$\sigma_{\Omega'=3/2}^\Omega / \sigma_{\Omega'=1/2}^\Omega = (3 + 3 \times a_2/a_0) / (3 - 5 \times a_2/a_0) \quad (9)$$

The contribution of each  $\Omega'$  component  $f_{\Omega'}^\Omega$  in the branching fraction  $f(\Omega)$  for the  $\text{RgX}^* (\text{B}, \Omega = 1/2)$  and  $\text{RgX}^* (\text{C}, \Omega = 3/2)$  to the  $\text{RgX}^* (\Omega)$  formation can be determined experimentally by using the  $a_2/a_0$  term as below

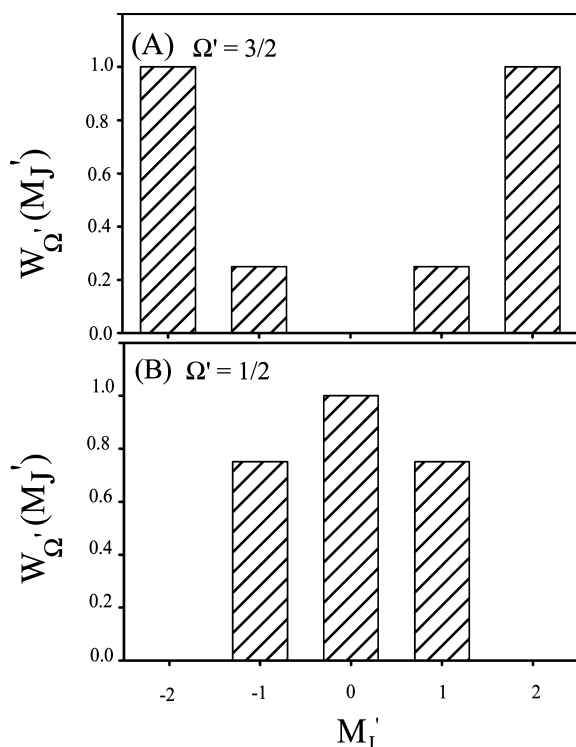


**Figure 3.**  $M'_j$  state dependence of each  $\Omega'$  component,  $W_{\Omega'}(M'_j)$ , for (A)  $\Omega' = 3/2$  and (B)  $\Omega' = 1/2$  calculated by using a standard recoupling procedure of angular momentum through the Clebsch-Gordan coefficients under the assumption that the angular momentum of the  $\text{Rg}^+ (^2\text{P}_{3/2})$  is conserved after the electron jump of the outer ns electron.

$$f_{\Omega'=1/2}^\Omega = \sigma_{\Omega'=1/2}^\Omega / (\sigma_{\Omega'=1/2}^\Omega + \sigma_{\Omega'=3/2}^\Omega) \times f(\Omega) \quad (10a)$$

$$= (3 - 5 \times a_2/a_0) / (6 - 2 \times a_2/a_0) \times f(\Omega)$$

$$f_{\Omega'=3/2}^\Omega = \sigma_{\Omega'=3/2}^\Omega / (\sigma_{\Omega'=1/2}^\Omega + \sigma_{\Omega'=3/2}^\Omega) \times f(\Omega) \quad (10b)$$

$$= (3 + 3 \times a_2/a_0) / (6 - 2 \times a_2/a_0) \times f(\Omega)$$

They are plotted in Figure 4 as a function of branching fraction  $f(\Omega)$  for each  $\text{RgX}^* (\Omega)$  channel to the  $\text{RgX}^* (\Omega)$  formation. The branching fraction  $f(\Omega)$  for each reaction system is cited from the refs 3–5. We can see a good linear relationship between  $f_{\Omega'}^\Omega$  and  $f(\Omega)$ . All experimental results can be expressed as follows

$$f_{1/2}^{3/2} = 0.375 \times f(\Omega = 3/2) + 0.02 \quad (11a)$$

$$f_{3/2}^{3/2} = 0.625 \times f(\Omega = 3/2) - 0.02 \quad (11b)$$

$$f_{1/2}^{1/2} = 0.625 \times f(\Omega = 1/2) - 0.095 \quad (11c)$$

$$f_{3/2}^{1/2} = 0.375 \times f(\Omega = 1/2) + 0.095 \quad (11d)$$

It is found that the slope for  $f_{3/2}^{3/2}$  is equal to that for  $f_{1/2}^{1/2}$ , whereas the slope for  $f_{1/2}^{3/2}$  is equal to that for  $f_{3/2}^{1/2}$ .

**3.3.  $\Omega_1$ -Conservation Model.** On the basis of the assumption that the  $\Omega'$  component is conserved in the course of ion-pair ( $\text{Rg}^+ - \text{RX}^-$ ) formation, the cross sections  $\sigma_{\Omega'=\Omega}^\Omega$  and  $\sigma_{\Omega' \neq \Omega}^\Omega$  in eq 9 should be determined by the following two factors.

Factor 1: Rotational coupling due to the change of the quantization axis from the collision frame to the ion-pair ( $\text{Rg}^+ - \text{RX}^-$ ) frame.

Factor 2: Dynamical effect in the eximer formation process, which is controlled by the  $\Omega_1$  component in the ion pair ( $\text{Rg}^+ (^2\text{P}_{3/2}) - \text{RX}^+$ ) frame.

Here we propose the  $\Omega_1$ -conservation model, in which a nonadiabatic switching of the quantization axis from the collision frame to the ion pair ( $\text{Rg}^+ (^2\text{P}_{3/2}) - \text{RX}^+$ ) frame is assumed at the distance  $R_{\text{ET}}$ , where the ion pair is formed via the electron transfer. A similar treatment in which different quantization axes are assumed for small and large separation has been reported in the context of atomic fine-structure-changing collisions.<sup>16–18</sup> In addition, the cross section for the  $\text{RgX}^* (\Omega)$  formation is assumed to be controlled by the  $\Omega_1$  component in the ion pair ( $\text{Rg}^+ (^2\text{P}_{3/2}) - \text{RX}^+$ ) frame. This model is schematically shown in Figure 5 for the case in which the ion pair ( $\text{Rg}^+ (^2\text{P}_{3/2}) - \text{RX}^-$ ) axis has an angle,  $\theta$ , against the collision frame of,  $\nu_{\text{R}}$ , because of the impact parameter  $b$ .

In this model, the cross section of  $\text{RgX}^* (\Omega)$  formation from the  $M'_j$  state at the angle  $\theta$  can be calculated by using Wigner's  $d$  function as follows<sup>15</sup>

$$\sigma^\Omega(\theta, M'_j) = \sum_{\Omega'} \sum_{\Omega_1} [\sigma_{\Omega_1 \rightarrow \Omega}(\theta) \times |d_{\Omega', \Omega_1}^{3/2}(\theta)|^2 \times W_{\Omega'}(M'_j)] \quad (12)$$

$$= [\sigma_{1/2 \rightarrow \Omega}(\theta) \times |d_{1/2, 1/2}^{3/2}(\theta)|^2 + \sigma_{3/2 \rightarrow \Omega}(\theta) \times |d_{1/2, 3/2}^{3/2}(\theta)|^2] \times W_{1/2}(M'_j)$$

$$+ [\sigma_{1/2 \rightarrow \Omega}(\theta) \times |d_{3/2, 1/2}^{3/2}(\theta)|^2 + \sigma_{3/2 \rightarrow \Omega}(\theta) \times |d_{3/2, 3/2}^{3/2}(\theta)|^2] \times W_{3/2}(M'_j)$$



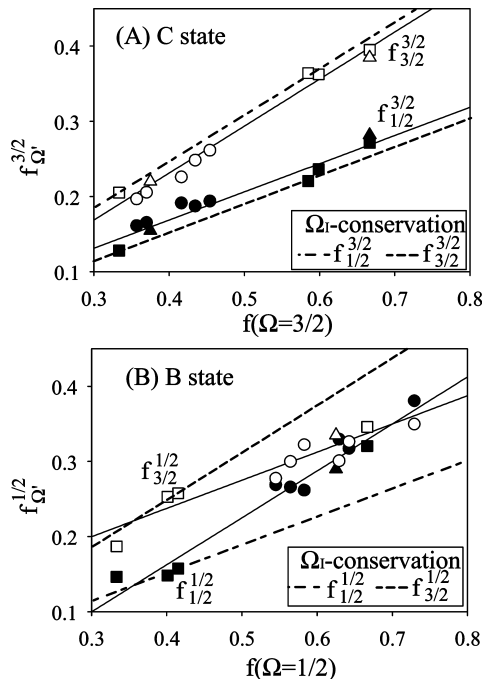


**Figure 4.** Contribution of each  $\Omega'$  component  $f_{\Omega'}^{\Omega}$  in the branching fraction  $f(\Omega)$  for the  $\text{RgX}^*$  (B,  $\Omega = 1/2$ ) and  $\text{RgX}^*$  (C,  $\Omega = 3/2$ ) formation. (A)  $\text{RgX}^*$  (C,  $\Omega = 3/2$ ); (B)  $\text{RgX}^*$  (B,  $\Omega = 1/2$ ). Experimental results obtained from eq 10a using the  $a_2/a_0$  term for Ar (triangle), Kr (square), and Xe (circle). (A)  $f_{3/2}^{3/2}$  (open symbol),  $f_{1/2}^{3/2}$  (closed symbol); (B)  $f_{3/2}^{1/2}$  (open symbol),  $f_{1/2}^{1/2}$  (closed symbol). Calculated values from eq 15a (dashed lines) under the  $\Omega_1$  conservation (solid lines) using the parameter of  $\sigma_{1/2-3/2}/\sigma^{\text{RgX}^*} = 0.075$ ,  $\sigma_{3/2-1/2}/\sigma^{\text{RgX}^*} = 0.375$ .

where  $\sigma_{\Omega_1-\Omega}(\theta)$  is the cross section for the  $\text{RgX}^*$  ( $\Omega$ ) formation from the  $\Omega_1$  component in the ion pair ( $\text{Rg}^+ (^2\text{P}_{3/2})-\text{RX}^+$ ) frame at the angle  $\theta$ . Therefore, the  $M_J$ -dependent cross section  $\sigma^{\Omega}(M_J)$  for  $\text{RgX}^*$  (B,  $\Omega = 1/2$ ) and  $\text{RgX}^*$  (C,  $\Omega = 3/2$ ) can be expressed by

$$\begin{aligned} \sigma^{\Omega}(M_J) = & [\langle \sigma_{1/2-\Omega}(\theta) \times |d_{1/2,1/2}^{3/2}(\theta)|^2 \rangle + \langle \sigma_{3/2-\Omega}(\theta) \times \\ & |d_{1/2,3/2}^{3/2}(\theta)|^2 \rangle] \times W_{1/2}(M_J) \\ & + [\langle \sigma_{1/2-\Omega}(\theta) \times |d_{3/2,1/2}^{3/2}(\theta)|^2 \rangle + \langle \sigma_{3/2-\Omega}(\theta) \times |d_{3/2,3/2}^{3/2}(\theta)|^2 \rangle] \times \\ & W_{3/2}(M_J) \end{aligned} \quad (13)$$

where the bracket represents the averaging over the angle  $\theta$  that depends on the impact parameter ( $b$ ) distribution.

To evaluate the effect due to factor 1, as an example, we consider the most simple case in which the isotropic electron transfer takes place at the constant intermolecular distance,  $R_{\text{ET}}$ , and the straight-line trajectories with a uniform impact parameter distribution over the range from 0 to  $R_{\text{ET}}$  are assumed. Moreover,  $\sigma_{\Omega_1-\Omega}(\theta)$  is assumed to have no  $\theta$  dependence, that is,  $\sigma_{\Omega_1-\Omega}(\theta) = \sigma_{\Omega_1-\Omega}$ . Figure 6 shows the  $\theta$ -dependence of the square of Wigner's  $d$  function  $|d_{\Omega_1,\Omega}^{3/2}(\theta)|^2$  in this simplest case.  $\langle |d_{\Omega_1,\Omega}^{3/2}(\theta)|^2 \rangle$  is calculated to be 0.625 and  $\langle |d_{\Omega_1,\Omega \neq \Omega}^{3/2}(\theta)|^2 \rangle$  is calculated to be 0.375. Finally, the cross sections can be expressed by

$$\begin{aligned} \sigma^{3/2}(M_J) = & [0.375 \times \sigma_{3/2-3/2} + 0.625 \times \sigma_{1/2-3/2}] \times \\ & W_{1/2}(M_J) \\ & + [0.625 \times \sigma_{3/2-3/2} + 0.375 \times \sigma_{1/2-3/2}] \times W_{3/2}(M_J) \end{aligned} \quad (14a)$$

$$\begin{aligned} \sigma^{1/2}(M_J) = & [0.625 \times \sigma_{1/2-1/2} + 0.375 \times \sigma_{3/2-1/2}] \times \\ & W_{1/2}(M_J) \\ & + [0.375 \times \sigma_{1/2-1/2} + 0.625 \times \sigma_{3/2-1/2}] \times W_{3/2}(M_J) \end{aligned} \quad (14b)$$

The total cross section  $\sigma^{\text{RgX}^*}$  for the  $\text{RgX}^*$  formation and the branching fraction  $f(\Omega = 3/2)$  and  $f(\Omega = 1/2)$  to each  $\Omega$  state can be defined as follows

$$\sigma^{\text{RgX}^*} = \sigma_{3/2-3/2} + \sigma_{1/2-3/2} + \sigma_{1/2-1/2} + \sigma_{3/2-1/2} \quad (15a)$$

$$f(\Omega = 3/2) = (\sigma_{3/2-3/2} + \sigma_{1/2-3/2})/\sigma^{\text{RgX}^*} \quad (15b)$$

$$f(\Omega = 1/2) = (\sigma_{1/2-1/2} + \sigma_{3/2-1/2})/\sigma^{\text{RgX}^*} \quad (15c)$$

Therefore, the contribution of each  $\Omega'$  component in the  $\text{RgX}^*$  (C,  $\Omega = 3/2$ ) and  $\text{RgX}^*$  (B,  $\Omega = 1/2$ ) state,  $f_{\Omega'}^{\Omega}$ , are summarized as below

$$f_{1/2}^{3/2} = (0.375 \times \sigma_{3/2-3/2} + 0.625 \times \sigma_{1/2-3/2})/\sigma^{\text{RgX}^*} \quad (16a)$$

$$= 0.375 \times f(\Omega = 3/2) + 0.25 \times \sigma_{1/2-3/2}/\sigma^{\text{RgX}^*}$$

$$f_{3/2}^{3/2} = (0.625 \times \sigma_{3/2-3/2} + 0.375 \times \sigma_{1/2-3/2})/\sigma^{\text{RgX}^*} \quad (16b)$$

$$= 0.625 \times f(\Omega = 3/2) - 0.25 \times \sigma_{1/2-3/2}/\sigma^{\text{RgX}^*}$$

$$f_{1/2}^{1/2} = (0.625 \times \sigma_{1/2-1/2} + 0.375 \times \sigma_{3/2-1/2})/\sigma^{\text{RgX}^*} \quad (16c)$$

$$= 0.625 \times f(\Omega = 1/2) - 0.25 \times \sigma_{3/2-1/2}/\sigma^{\text{RgX}^*}$$

$$f_{3/2}^{1/2} = (0.375 \times \sigma_{1/2-1/2} + 0.625 \times \sigma_{3/2-1/2})/\sigma^{\text{RgX}^*} \quad (16d)$$

$$= 0.375 \times f(\Omega = 1/2) + 0.25 \times \sigma_{3/2-1/2}/\sigma^{\text{RgX}^*}$$

These expressions are in agreement with the experimental ones (eqs 11a–11d). The experimental results in Figure 4 can be well represented by eqs 16a–16d using the following parameters (see solid lines in Figure 4)

$$\sigma_{1/2-3/2}/\sigma^{\text{RgX}^*} = 0.075, \quad \sigma_{3/2-1/2}/\sigma^{\text{RgX}^*} = 0.375 \quad (17)$$

That is, the fraction of the  $\Omega_1$ -changing process in the  $\text{RgX}^*$  formation has no dependence on the reactant and Rg.

Needless to say, the calculated result depends on the parameters used in the model. To calculate the true cross section, one has to take into account the  $b$ -dependent electron transfer probability and the actual particle trajectories. However, in the present reaction system, it is not unreasonable to assume that

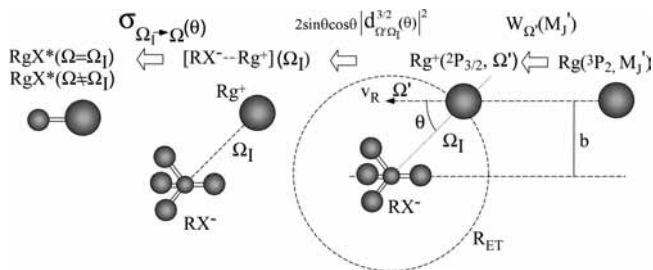


**Figure 5.** Schematic drawing of the  $\Omega_1$  conservation model. The electron transfer process is assumed to be isotropic and takes place at the constant intermolecular distance,  $R_{ET}$  (dashed circle). Straight-line trajectories with uniform impact parameter  $b$  distribution are assumed. For a collision with impact parameter  $b$ , the direction of the ion pair ( $\text{Rg}^+ (^2\text{P}_{3/2}, \Omega_1) - \text{RX}^-$ ) frame has the angle,  $\theta$ , against the relative velocity vector,  $v_R$ , in the collision frame. Conservation of the ion core  $\text{Rg}^+ (^2\text{P}_{3/2}, \Omega')$  is assumed in the course of the electron jump of the  $ns$  electron. The cross section for the  $\text{RgX}^* (\Omega)$  formation is assumed to be controlled by the  $\Omega_1$  component in the ion-pair ( $\text{Rg}^+ (^2\text{P}_{3/2}, \Omega_1) - \text{RX}^-$ ) frame that can be determined by using Wigner's  $d$  function. The cross section for the  $\text{RgX}^* (\Omega)$  formation from the  $\Omega_1$  configuration at the angle of  $\theta$  is shown as  $\sigma_{\Omega_1 \rightarrow \Omega}(\theta)$ .

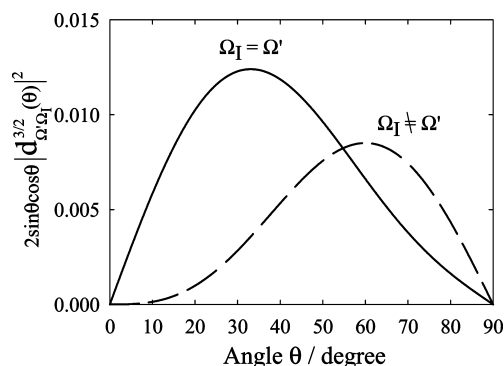


**Figure 6.**  $\theta$ -dependence of Wigner's  $d$  function  $|d_{\Omega_1, \Omega}^{3/2}(\theta)|^2$  for the simplest case, in which the isotropic electron transfer takes place at the constant intermolecular distance,  $R_{ET}$ , and straight-line trajectories with a uniform impact parameter distribution are assumed. Collisions with a small impact parameter dominantly contribute to the  $\Omega_1 = \Omega'$  process, whereas collisions with a large impact parameter dominantly contribute to the  $\Omega_1 \neq \Omega'$  process. The square of Wigner's  $d$  function  $|d_{\Omega_1, \Omega}^{3/2}(\theta)|^2$  averaged over the angle  $\theta$  becomes  $\langle |d_{\Omega_1, \Omega}^{3/2}(\theta)|^2 \rangle = 0.625$  and  $\langle |d_{\Omega_1, \Omega}^{3/2}(\theta)|^2 \rangle = 0.375$ .

isotropic electron transfer takes place at the constant intermolecular distance  $R_{ET}$  with the straight-line trajectories because the electron transfer process for the formation of ion pair ( $\text{Rg}^+ - \text{RX}^-$ ) has little atomic alignment effect. Moreover, the estimated  $R_{ET}$  from the total quenching rate constant is expected to be large enough to assume straight-line trajectories with little effect from the intermolecular potential. Although the calculated result is only an indication of to what extent the  $\Omega'$  population in the collision frame can couple to the  $\Omega_1$  population in the ion-pair ( $\text{Rg}^+ - \text{RX}^-$ ) frame by factor 1, the calculated results are in good agreement with the experimental results, indicating the importance of rotational coupling (factor 1) in the excimer formation. It is strongly suggested that the atomic alignment effect for the excimer formation is dominantly controlled by factor 1 (rotational coupling due to the change of quantization axis). In particular, the atomic alignment effect for the  $\text{RgX}^*$  (C,  $\Omega = 3/2$ ) formation can be explained only by the  $\Omega_1$  conservation through the  $\text{RgX}$  formation from the ion pair

( $\text{Rg}^+ - \text{RX}^-$ ) without considering dynamical effect, that is,  $\sigma_{1/2 \rightarrow 3/2} / \sigma^{\text{RgX}^*} \approx 0$ . However, according to this model calculation, only the formation of  $\text{RgX}^*$  (B,  $\Omega = 1/2$ ) is significantly affected by the dynamics upon the exit potential. In other words, the collision under the  $|M_J| = 2$  configurations of  $\text{Rg} (^3\text{P}_2)$  with a small impact parameter is unusually reactive for the  $\text{RgX}^*$  (B,  $\Omega = 1/2$ ) formation without the conservation of the  $\Omega_1$  component in the ion-pair ( $\text{Rg}^+ - \text{RX}^-$ ) frame. In this case, the fraction of the cross section for the  $\Omega_1$ -changing process has no dependence on the target reactant  $\text{RX}$  and  $\text{Rg}$ .

#### 4. Conclusions

The atomic alignment effect for the formation of  $\text{RgX}^*$  (B, C) in the reaction of  $\text{Rg} (^3\text{P}_2) + \text{RX}$  has been measured by using the oriented  $\text{Rg} (^3\text{P}_2, M_J = 2)$  beam at a collision energy of  $\sim 0.07$  eV. The reactant (RX) dependence of the atomic alignment effect is extremely different between the  $\text{RgX}^*$  (B) and  $\text{RgX}^*$  (C) channels. For the  $\text{RgX}^*$  (C) channel, an analogous atomic alignment effect is commonly observed despite the different RX. In contrast, for the  $\text{RgX}^*$  (B) channel, the atomic alignment effect shows a diverse dependence on RX and Rg. An  $\Omega_1$  conservation model, which is based on the conservation of  $\Omega'$  component in the course of ion-pair ( $\text{Rg}^+ - \text{RX}^-$ ) formation, is proposed. According to the  $\Omega_1$  conservation model, it is suggested that the atomic alignment effect for the  $\text{RgX}^*$  (C,  $\Omega = 3/2$ ) formation is dominantly controlled by the  $\Omega_1$  distribution in the ion-pair ( $\text{Rg}^+ - \text{RX}^-$ ) frame. The collisions under the  $|M_J| = 2$  configurations of  $\text{Rg} (^3\text{P}_2)$  with the small impact parameters can produce the  $\text{RgX}^*$  (B,  $\Omega = 1/2$ ) without following the  $\Omega_1$  conservation because of the dynamical effect in the excimer formation process from the ion pair ( $\text{Rg}^+ - \text{RX}^-$ ).

#### References and Notes

- (1) Setser, D. W.; Dreiling, T. P.; Brashers, H. C.; Kolts, J. H. *Faraday Discuss. Chem. Soc.* **1979**, *67*, 255.
- (2) Riley, S. J.; Siska, P. E.; Herschbach, D. R. *Faraday Discuss. Chem. Soc.* **1979**, *67*, 27.
- (3) Tamagake, K.; Setser, D. W.; Kolts, J. H. *J. Chem. Phys.* **1981**, *74*, 4286.
- (4) Kolts, J. H.; Velazco, J. E.; Setser, D. W. *J. Chem. Phys.* **1979**, *71*, 1247.
- (5) Sadeghi, N.; Cheaib, M.; Setser, D. W. *J. Chem. Phys.* **1989**, *90*, 219.
- (6) Zhong, D.; Setser, D. W.; Sobczynski, R.; Gadomski, W. *J. Chem. Phys.* **1996**, *105*, 5020.
- (7) Velazco, J. E.; Kolts, J. H.; Setser, D. W. *J. Chem. Phys.* **1976**, *65*, 3468.
- (8) Tsuji, M.; Furusawa, M.; Nishimura, Y. *J. Chem. Phys.* **1990**, *92*, 6502.
- (9) Rettner, C. T.; Zare, R. N. *J. Chem. Phys.* **1982**, *77*, 2416.
- (10) Yang, W. S.; Ding, G. W.; Xu, D. I.; Sun, W. Z.; Gu, Y. S.; He, G. Z.; Lou, N. Q. *J. Chem. Phys.* **1995**, *103*, 345.
- (11) Suits, A. G.; Hou, H.; Davis, H. F.; Lee, Y. T. *J. Chem. Phys.* **1992**, *96*, 2777.
- (12) Yasuda, K.; Ohoyama, H.; Kasai, T. *J. Phys. Chem. A* **2008**, *112*, 11543.
- (13) Watanabe, D.; Ohoyama, H.; Matsumura, T.; Kasai, T. *J. Chem. Phys.* **2006**, *125*, 084316.
- (14) Watanabe, D.; Ohoyama, H.; Matsumura, T.; Kasai, T. *Phys. Rev. Lett.* **2007**, *99*, 043201.
- (15) Zare, R. N. *Angular Momentum*; Wiley, New York, 1998.
- (16) Mies, F. H. *Phys. Rev. A* **1973**, *7*, 942.
- (17) Aquilanti, V.; Casavecchia, P.; Grossi, G.; Lagana, A. *J. Chem. Phys.* **1980**, *73*, 1173.
- (18) Aquilanti, V.; Luzzatti, E.; Pirani, F.; Volpi, G. G. *J. Chem. Phys.* **1980**, *73*, 1181.